



Dexterity optimization by port placement in robot-assisted minimally invasive surgery

Citation

Selha, Shaun, Pierre Dupont, Robert Howe, and David Torchiana. 2001. "Dexterity optimization by port placement in robot-assisted minimally invasive surgery." SPIE International Symposium on Intelligent Systems and Advanced Manufacturing, Newton, MA, October 28-31, 2001.

Published version

<https://doi.org/10.1117/12.454734>

Link

<http://nrs.harvard.edu/urn-3:HUL.InstRepos:33892601>

Terms of use

This article was downloaded from Harvard University's DASH repository, and is made available under the terms and conditions applicable to Other Posted Material (LAA), as set forth at

<https://harvardwiki.atlassian.net/wiki/external/NGY5NDE4ZjgzNTc5NDQzMGIzZWZhMGFIOWI2M2EwYTg>

Accessibility

<https://accessibility.huit.harvard.edu/digital-accessibility-policy>

Share Your Story

The Harvard community has made this article openly available.
Please share how this access benefits you. [Submit a story](#)

Dexterity optimization by port placement in robot-assisted minimally invasive surgery

Shaun Selha¹, Pierre Dupont¹, Robert Howe², David Torchiana³

¹ Aerospace and Mechanical Engineering, Boston University, Boston MA, USA;

² Division of Engineering and Applied Science, Harvard University, Cambridge MA, USA;

³ Division of Cardiac Surgery, Massachusetts General Hospital, Boston MA, USA

ABSTRACT

A computer-based algorithm has been developed which uses preoperative images to provide a surgeon with a list of feasible port triplets ranked according to tool dexterity and endoscopic view quality at each surgical site involved in a procedure. A computer simulation allows the surgeon to select from among the proposed port locations. The procedure selected for the development of the system consists of a coronary artery bypass graft (CABG). In this procedure, the interior mammary artery (IMA) is mobilized from the interior chest wall, and one end is attached to the coronary arteries to provide a new blood supply for the heart. Approximately 10-20 cm is dissected free, using blunt dissection and a harmonic scalpel or electrocautery. At present, the port placement system is being evaluated in clinical trials.

Keywords: Port Placement, Dexterity, Minimally Invasive Surgery, Telesurgery.

1. INTRODUCTION

Robotic assistance enables the use of minimally invasive techniques in coronary artery bypass grafting by scaling hand motions, decreasing tremor, and enhancing manipulation. In these procedures, endoscopes and other instruments are inserted through small incisions or “ports” to access the surgical site. In initial trials of this approach, inappropriate port locations have posed a number of difficulties including poor tool dexterity, an inability to reach all the required surgical sites, and an increased likelihood of collision between the instruments, both within and outside the patient’s body.

This paper presents an algorithm for optimizing port placement for the ZEUSTM surgical robot system. The three main issues in defining optimal port placement are tool dexterity, endoscopic viewpoint, and workspace limits. Tool dexterity is defined by the relative orientation of the tools with respect to each other and the surgical site. Endoscopic viewpoint is defined with respect to the tools and with respect to the surgical site. Workspace limits are reached when a desired tool motion would cause a tool/ endoscope/ patient collision (internal) or a robot/ robot/ patient collision (external).

2. BACKGROUND

Several medical research groups have addressed the problem of optimal port placement for robotically assisted minimally invasive surgery, with respect to tool dexterity, endoscopic viewpoint, and workspace limits¹⁻³. Coste-Maniere et al. have presented a pre-operative planning and simulation system for minimally invasive surgery using the daVinciTM robot system^{1,2}. The approach consisted of a planning, validation and simulation phase. Criteria considered in the port location process included the surgical target site, the attack angle of the instrument, describing the angle between a normal to the surgical site and the instrument, and a dexterity parameter, describing the angle between the surface normal of the port and the instrument. Optimal angles were based on the experience of a cardiac surgeon. In this approach, possible port locations for two instruments and an endoscope are ranked according to these criteria as well as the potential for external robot collisions.

Contact information: Shaun Selha (busds@bu.edu), Pierre Dupont (Pierre@bu.edu),
Robert Howe (howe@deas.harvard.edu), and David Torchiana (dtorchiana@partners.org)

Experimental guidelines for the selection of port locations for the ZEUS™ robot system made by Computer Motion, Inc. are presented by H. Tabaie et al.³. Based on dry lab experiments, a template was developed indicating optimal robot configurations as well as ideal instrument and endoscope port locations. A port template diagram defines the optimal relative locations and orientations of the right and left instruments and the endoscope. A similar diagram is employed here and will be presented in section 3.

Within the robotics literature, the issues of tool dexterity, endoscopic viewpoint, and workspace limits can be related to robot dexterity⁴⁻¹⁰. Many of the reported dexterity measures have been proposed to measure endpoint dexterity for multi-link robots. Consequently they involve some function of the singular values of the Jacobian matrix, thus penalizing robot arm configurations for which end point translations and rotations require large joint motions. The most referenced of these is the manipulability measure proposed by Yoshikawa⁴, which is defined as the square root of the determinant of the matrix JJ^T . This is simply the product of the singular values of J . Other proposed measures include the minimum singular value of the Jacobian, which was proposed by Klein and Blaho⁵, as well as the trace of the matrix JJ^T , put forth by Baillieul⁶. Other measures include the compatibility index formulated by Chiu⁷, and isotropy (all equal singular values) proposed by Salisbury and Craig⁸.

An alternate approach to defining dexterity is the joint range availability function first proposed by Liegeois⁹. In this approach, dexterity is highest when joints are centered in specified ranges. This approach has been recently augmented by Liang and Liu¹⁰ such that the desired midrange angle of each joint is switched at a series of pre-specified path points of the end effector. They also proposed applying variable weightings to the angles in order to achieve the proper postures effectively.

In the next section, the port placement problem is defined and the appropriate approach to measuring dexterity is explained. In the following section, an overall dexterity metric incorporating tool dexterity, endoscopic viewpoint and workspace limits is formally defined, which is related to joint range availability. Implementation of the algorithm is detailed in section 5 and the last sections describe ongoing clinical trials and assessment goals.

3. PROBLEM DEFINITION – PORT PLACEMENT

In the minimally invasive surgical procedures considered here, three thin rods are inserted into the patient's thorax through separate incisions in the chest wall, called ports. These incisions are made in the intercostal spaces, i.e., between the ribs. Two of these rods constitute instruments and terminate, interior to the patient, with tools, such as a gripper, scalpel or cauterizing tool. The third rod is an endoscope, providing a camera view of the surgical site. In the Zeus™ system, there is no articulation at the distal ends of the rods where the tools attach. There are often, however, fixed offset angles between a rod's axis and its tool or endoscope.

The proximal end of the rod is attached, exterior to the patient, to a six degree of freedom robot with four active joints and two passive joints. The ports act as fulcrums for the rods. Motions of a tool or endoscope are accomplished solely by translations of the rod along its axis and rotations of the rod about its port.

The robots are clamped to the operating table and include two additional locking joints. By adjusting the clamping position of the robot relative to the surgical table and by adjusting the two locking joints, the robot can be configured relative to the surgical table and patient.

Dexterity-related difficulties during surgery can be attributed to the following factors:

1. Inability to reach the surgical site,
2. Inability to perform the surgical procedure due to the orientations of the tools with respect to each other and the surgical site,
3. Instrument/endoscope collisions occurring inside the body,
4. Robot singularities and joint limits, and
5. Robot collisions.

The approach taken in this paper is to decompose the overall dexterity problem into two sub-problems: port placement and robot placement. Port placement deals with difficulties 1-3 while robot placement controls difficulties 4-5. By employing this decomposition, the problem of port placement can be addressed independently in this paper. The port locations so obtained can be combined with a robot positioning solution based on either experience or an algorithm developed for the purpose.

By decoupling the problems of port and robot placement, the overall dexterity problem is also decoupled. Consideration of difficulties 1-5 above indicates that different dexterity measures may be appropriate to each sub-problem. Only port placement dexterity is considered here. The metric described in the following sections was developed through surgical observation and interview.

3.1 Port placement coordinates

The coordinate frame and relative angles used to define port placement dexterity are shown in Figure 1. For clarity, only the cylindrical rods of the instruments and endoscope are depicted along with a small planar patch representing the surgical site. A coordinate frame is defined relative to the surgical site such that the y -axis is normal to the site. For the procedures described here, the normal is always considered to be oriented vertically. In this case, the axes can be further specified such that the x -axis is taken to be parallel to the patient's spine, and, together with the z -axis, lies in a plane parallel to the operating table.

The angles used to define the positions of the right and left instruments and the endoscope, each held by their respective robotic arms, can be described relative to this coordinate frame as shown in Figure 1. The two instruments lie in a plane (the instrument plane) with angle of elevation γ from the z -axis. Within the tool plane, the left and right instruments are oriented at angles θ_l and θ_r with respect to the negative and positive x -axis, respectively.

Endoscope orientation is described by three angles, ϕ_e, ϕ_a, ϕ_o . The first two, ϕ_e and ϕ_a , are elevation and azimuthal angles of the endoscope, respectively. Not depicted, ϕ_o is a constant offset angle between the endoscope's axis and its line of sight. In the procedures under consideration, a 30-degree offset endoscope is typically used.

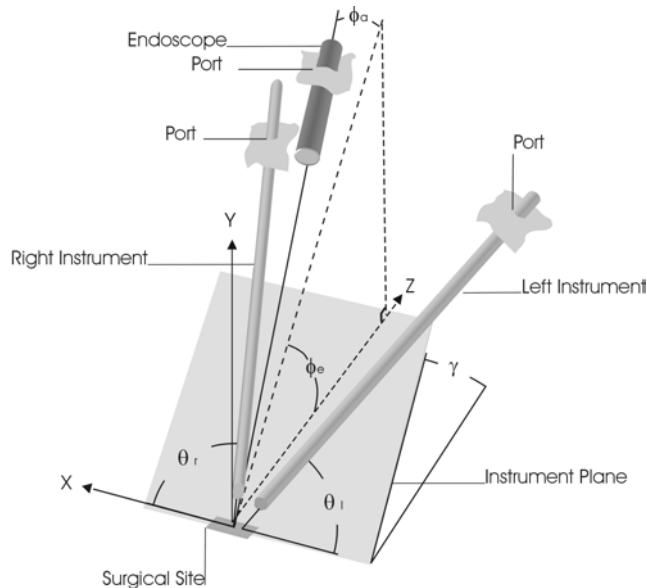


Figure 1: Model System

4. DEXTERITY FUNCTION

An overall dexterity metric, D , addressing tool dexterity, endoscopic viewpoint and workspace limits, can be defined in a manner similar to joint range availability:

$$D = w^T \sum_{i=1}^n (\psi_i - \psi_{\text{opt}})^2 \quad (1)$$

Here, w is a weighting vector, $\psi_i = [\theta_r; \gamma_r; \theta_l; \gamma_l; \varphi_e; \varphi_a]^T$ is the vector of instrument and endoscope orientation angles at the i^{th} surgical site and ψ_{opt} is the vector of optimal orientation angles. As a metric, it measures, over all surgical sites, the average “distance” squared of instruments and endoscope from their optimal orientations. The values used for ψ_{opt} and w appear in Table 1 and are based on the experience of the fourth author performing numerous open- and closed-chest procedures.

Angle	Weighting Factor	ψ_{opt} , degrees IMA Take-Down	ψ_{opt} , degrees Anastomosis
θ_r	0.35	60	60
γ_r	0.25	-20	45
θ_l	0.35	60	60
γ_l	0.25	-20	45
φ_e	0.25	7	52
φ_a	0.15	0	0

Table 1: Weighting Factors and Optimal Angles (Endoscope offset angle $\varphi_o = 30^\circ$).

A qualitative explanation of the optimal angles can be given as follows. The relative orientation of the instruments and endoscope in Figure 1 is motivated by the desire to make robotic surgery intuitive. This is accomplished by preserving the relative orientations of the surgeon’s hands and eyes with respect to the surgical site, as displayed on a video screen. Thus, the left and right instruments are constrained to share the same optimal angle of elevation, $\gamma_r = \gamma_l$. The optimal values are due to the relative anatomical locations of the IMA and heart since the same ports must be used for IMA mobilization (takedown) and anastomosis.

Intuitiveness also constrains the endoscope to be positioned between the left and right instruments. Furthermore, experience has shown that minimizing φ_a (i.e., $\varphi_{a,\text{opt}} = 0$) minimizes the length of the endoscope inserted into the patient’s thorax. This in turn minimizes the probability of an internal collision between the endoscope and the right and left instruments.

The endoscope elevation angles, not including offset, are 7 degrees for IMA takedown and 52 degrees for anastomosis. In viewing the IMA, which runs along the underside of the sternum, the 7 degree elevation angle combines with the 30 degree offset to look upward at an angle of 22 degrees. During takedown, the instruments are also angled upward and must move through a large range of travel to the left and right. Achieving a viewing angle steeper than 22 degrees would necessitate insertion of a greater length of endoscope, which would generate collisions with the instruments.

For anastomosis, the 52 degree elevation angle combines with the 30 degree offset to achieve an 82 degree viewing angle. While an optimal viewing angle of 90 degrees could be achieved, the 8 degree offset makes it possible to flush the endoscope lens from an assist port during the procedure.

Among the orientation angles, experience dictates that the order of importance is θ_r and θ_l , followed by γ_r , γ_l , and φ_e , and then by φ_a . This indicates that the position of the surgical instruments is more critical than the position of the endoscope. The values of the weighting factors in Table 1 were chosen accordingly. Note that the optimal angles and weighting factors can be modified for other procedures or the preferences of other surgeons.

5. IMPLEMENTATION

5.1 Algorithm

A search algorithm and graphical user interface have been developed using the dexterity function of (1). The inputs and outputs of the system are listed in Table 2. For the planning to be based on a specific patient's anatomy, a preoperative CT scan is required with a contrast agent used for artery imaging. The image must be segmented to obtain 3D models of the skin, rib cage, IMA and heart. Additional inputs include the type of procedure, a set of targeted surgical sites and a grid of feasible port locations.

Inputs	Outputs
1. Preoperative CT image	1. List of dexterity-ranked port triplets
2. Type of procedure (IMA takedown, anastomosis)	2. Dexterity grids
3. Set of surgical sites	
4. Grid of feasible port locations	

Table 2: Algorithm inputs and outputs.

The user selects a set of surgical sites and a grid of feasible port locations using a computer mouse to interact with the 3D models through a graphical interface. The grid of port locations is selected using the skin model and must be located in the intercostal spaces, i.e., between the ribs. For IMA takedown, four target sites, spanning the length of artery to be harvested, are specified. For anastomosis, a single target location must be specified for the coronary artery to be bypassed. As shown in Figure 1, surgical sites are defined by a point in space and a surface normal. In the current implementation, the normal is assumed to be in the positive y -axis direction for anastomosis, and in the negative y -axis direction for IMA takedown. In both cases the normal is perpendicular to the surgical table.

For both procedures, the algorithm combines feasible port locations into triplets (for the left and right instruments and endoscope). Feasible port triplets correspond to a subset of array triplets that fall within the workspace limits, meet the minimum dexterity and viewing requirements, and satisfy the surgeon's preferences. The feasible triplets are ranked using the dexterity function through an exhaustive search. Algorithm outputs consist of the ranked list of triplets and dexterity grids. The latter are three arrays corresponding to the endoscope and left and right instruments. Each array provides a dexterity ranking of the entire grid of feasible ports for its instrument or endoscope. Display of the outputs and operator interaction are described in the next section on visualization.

5.2 Visualization for surgical planning

After the port triplets are ranked, a graphical display is utilized to evaluate them. The graphical display consists of a virtual interactive environment that, at the user's discretion, displays any combination of the heart, IMA, rib cage, skin and feasible port grid. The surgical instruments and endoscope can be displayed at any of the ranked feasible port triplets. In addition, the viewpoint can be changed through rotation and scaling to improve visualization. Figure 3 depicts several possible views.

The display window can be switched between the external view of Figure 3 and the view of the endoscope. The instruments and endoscope can be manipulated through keyboard commands to evaluate dexterity at any surgical site as well as to test the range of motion and the endoscope view.

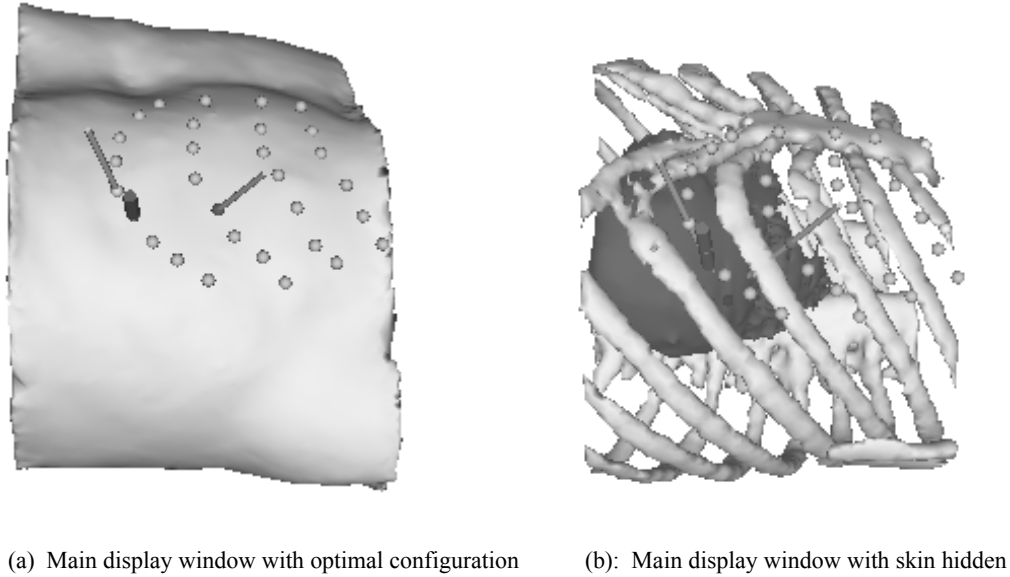


Figure 3

Three additional display windows depict the dexterity grid for the two instruments and the endoscope. These displays show the grid of feasible port locations color- and brightness-coded according to the dexterity metric. Color indicates deviation of port orientation from the optimal primary angle while brightness indicates deviation from the optimal secondary angle. For the right and left instruments, the primary angle is θ and the secondary angle is γ . For the endoscope, the primary angle is φ_e , and the secondary angle is φ_d . This feature is useful for directing the search of a user who wishes to evaluate a neighborhood of port triplets.

5.3 Operating room registration

Once a port triplet is evaluated and selected, the locations of the ports must be transferred to the patient in the operating room. To minimize the effect of body motions, the preoperative image must have been taken with the patient in the same body posture as is used on the surgical table. To perform registration between the preoperative image and the patient, an electromagnetic tracking system is used to measure the operating room coordinates of three anatomical landmarks on the patient. The same landmarks are identified in the solid model using the graphical interface. The landmarks selected usually consist of the xiphoid process, the top notch of the sternum and a rib or clavicle.

The transformation relating model and operating room coordinates is then computed. It consists of scaling, translation and rotation. Using this transformation, the desired port locations can be expressed in the coordinate system of the operating room tracking system. For each port, the position error between the tracking sensor's coordinates and the desired port are displayed. The operator moves the sensor to the body position indicating zero error and marks the spot for port insertion. This is repeated for all ports.

5.4 System evaluation

An evaluation protocol is currently being developed for in vitro and in vivo trials. Several questions will be posed in these studies. The first question is whether port locations are statistically different when selected by the algorithm and by

the existing template method. Geometric measures, such as the dexterity metric and Euclidean distance, will be used to compute the difference between port triplets. Additional measures will be based on surgeon performance of specially designed evaluation tasks. One such measure would be the time to touch a sequence of markers along the IMA.

A second question is whether the graphical interface is effective for evaluating potential port locations. This question can be addressed statistically by having a surgeon utilize the graphical interface to perform the same evaluation tasks that he performs in vivo. The relationship between the time taken in the two modalities, as well as the collisions experienced and surgeon preferences, can then be compared.

6. CONCLUSIONS

Port placement optimization is being investigated with the goals of increasing surgeon dexterity and decreasing procedure duration. In stopped heart procedures, the latter means less time on cardiopulmonary bypass, thus reducing its associated complications. The assessment methods described above are currently being used to evaluate the algorithm. The benefits so identified must be weighed against the costs involved in using the proposed system. These include hardware and software costs, preoperative imaging and model segmentation costs, as well as the surgeon's time.

Patients requiring these procedures are often overweight and so current templates developed for the anatomy of fit subjects will likely be inadequate. The long-term utility of the port placement system, however, will likely hinge on the variation with human anatomy of acceptable port locations in the population indicating CABG. Alternately, the system may serve as a useful training tool for surgeons learning to perform minimally invasive procedures.

Upcoming in vivo trials will answer these questions, and provide insight into the need for system modifications. In addition, these trials will provide clues regarding the importance of conducting future work on the optimization of robot placement and arm posture.

REFERENCES

1. L. Adhami, E. Coste-Maniere and J.D. Boissonnat, Planning and simulation of robotically assisted minimally invasive surgery. *Proc MICCAI '00*. Lecture notes in computer science. Vol. 1935, Springer, October 2000.
2. E.Coste-Maniere, L.Adhami, R. Severac-Bastide, A. Lobontiu, J. Salsibury Jr., J. D. Boissonnat, N. Swarup, G. Guthart, E. Mousseauz and A. C. Carpentier, Optimized port placement for the totally endoscopic coronary artery bypass grafting using the daVinci robotic system. *Proc. Intl. Symp. Exp. Rob.* Springer, December 2000.
3. H. Tabaie, J. Reinbolt, W. Graper, T.Kelly and M. Connor, Endoscopic coronary artery bypass graft (ECABG) procedure with robotic assistance, *Heart Surgery Forum* # 1999-0552, 2:310-317, 1999.
4. T.Yoshikawa, Manipulability of robotic mechanisms, *Int. J. Robotics Res.*, vol. 4, no. 2, pp. 3-9, 1985.
5. C.A. Klein and B.E. Blaho, Dexterity measures for the design and control of kinematically redundant manipulators, *Int. J. Robotics Res.* vol 6, no. 2, pp. 72-83, 1987.
6. J. Baillieul, A constrained oriented approach to inverse problems for kinematically redundant manipulators, *Proc. IEEE Int. Conf. On Robotics and Automation*, pp. 1827-1833, 1987.
7. S.L. Chiu, Control of redundant manipulators for task compatibility, *Proc. IEEE Int. Conf. On Robotics and Automat.*, pp. 1718-1724, 1987.
8. J.K. Salisbury and J.T. Craig, Articulated hands: force control and kinematic issues, *Int. J. Robotics Res.*, vol 1, no. 1, pp. 4-17, 1982.

9. A. Liegeois, Automatic supervisory control of the configuration and behavior of multibody mechanisms, *IEEE Trans. Syst., Man, Cybernetics.*, vol SMC-7, no. 12, Dec., pp. 868-871, 1977.
10. T.C. Liang and J.S. Liu, An improved trajectory planner for redundant manipulators in constrained workspace, *Proc. IEEE Int. Conf. On Robotics and Automation*, pp. 3153-3158, 1999.
11. R. Kikinis, , F. Jacobson, J. Kettenbach, and M. Sweeney, *Virtual human models*, Brigham and Women's Hospital, Boston, MA
12. J. White and J. Titus, Massachusetts General Hospital, Division of Cardiac Surgery, Dr. David Torchiana's Research Laboratory, Boston, MA